Automated Droplet Manipulation through Electrowetting on Dielectric for Solid-Phase Oligonucleotide Synthesis

Hee Tae An, Dr. Michael Schertzer

***Abstract*—Electrowetting on dielectric (EWOD) discrete microfluidic (DMF) devices have shown favorable properties for use in microreactor lab-on-a-chip applications. The following work looks toward the design and fabrication of EWOD devices for the automated droplet manipulation necessary in the ultimate goal of oligonucleotide synthesis. By modifying the previous work on mechanical filtration on EWOD devices by Schertzer et al. to be compatible with processing in the RIT Semiconductor & Microsystems Fabrication Laboratory, DI water droplets were successfully able to be moved from electrode to electrode or created from reservoir electrodes using a gap between devices of approximately 100 - 250 μm with a generated 1 kHz and 35.5 V_{rms} sinusoidal signal. Though much work will be necessary to enable oligonucleotide synthesis, the baseline work verified the functionality of key manipulation functions and and manipulation automation for the first time at the RIT Discrete Microfluidic Laboratory.**

***Index Terms*—discrete microfluidics, microfluidics, electrowetting on dielectric, EWOD, electrowetting, oligonucleotide synthesis, lab-on-a-chip.**

I. Introduction

DISCRETE microfluidic devices have been the focus of much developmental research and industrial use as an on-chip solution for many applications through the automated rapid manipulation of droplets with volumes between a micro and nanoliter [1]. As a relatively inexpensive and simple lab-on-a-chip to fabricate, this technology has garnered much attention in the biomedical industry as a platform for oligonucleotide synthesis. Previous work by Lee et al. utilized a continuous microfluidic device which employed a system of microfabricated channels in order to perform solid phase oligonucleotide synthesis [2]. While these devices were successfully able to perform synthesis, this passive manipulation method relies on external and difficult to maintain control systems that often tend to be slow and inefficient especially in large-array applications. More recent work by Schertzer et al. have demonstrated the manipulation and filtration of particles immersed in droplets through the used of an active method referred to as electrowetting on dielectric (EWOD) [3]. As this movement method shows more favorable performance in throughput and power consumption, the following work will look toward the device fabrication and manipulation automation of droplets as preliminary research for performing oligonucleotide synthesis.

Hee Tae An is a student at Rochester Institute of Technology in the Department of Electrical and Microelectronic Engineering.

Advisor Dr. Michael Schertzer is a professor at Rochester Institute of Technology in the department of Mechanical Engineering.

II. Theory

A. Solid Phase Oligonucleotide Synthesis

Oligonucleotides are a short chain of nucleobases (adenine, cytosine, guanine, thymine, and uracil) that are sequenced in a particular combination for various applications. Initial works in oligonucleotide synthesis was conducted through the use of synthetic analogs of naturally occurring molecules known as H-phosphonates. Because of their inherent low reactivity and subsequent low yield, synthesis was eventually performed using nucleoside phosphoramidites which greatly increase the rate of coupling between nucleosides [4]. In order to control the synthesis process, a dimethoxytrityl (DMT) protecting molecule is attached to the nucleoside phosphoramidite. With the ability to remove these protecting DMT groups through relatively mild acid reactions, oligonucleotides are synthesized through the coupling of a protected nucleoside molecule to an deprotected molecule.

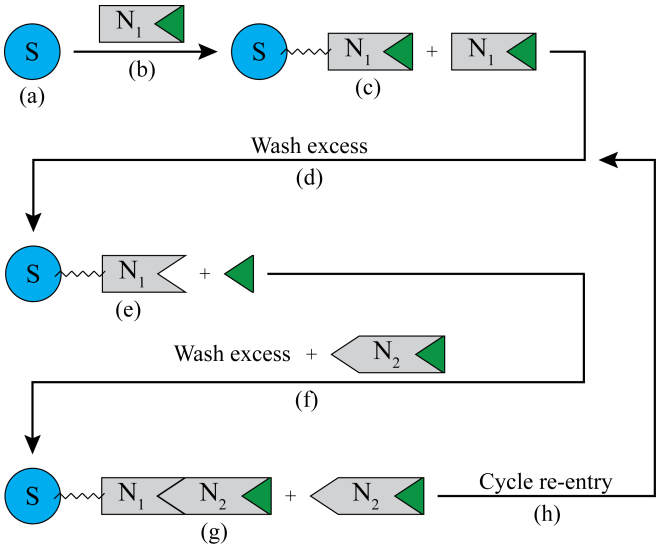

Figure 1. Overview of solid-phase oligonucleotide synthesis process.

Figure 1 depicts a simplified process flow for solid phase oligonucleotide synthesis: (a) introduction of the solid-support material at reaction site, (b) introduction of protected nucleoside molecule, (c) reactive attachment of nucleoside molecules to the solid-support material, (d) washing away of non-reacted

molecules from reaction site, (e) detritylation of protected nucleosides, (f) washing away of unattached protection groups and introduction of additional protected nucleoside molecules from reaction site, (g) reactive attachment of nucleoside molecules to the previous detritylated nucleosides, and (h) reentry into synthesis cycle at washing step (d).

The most important challenge in enabling this synthesis process comes from manipulation of either liquid reactants or solid reactants immersed in liquid. Due to this notion, a reliable method for manipulating liquids is required to achieve rapid synthesis. Additionally, as this synthesis process relies on the constant washing of excess reactant from the reaction site, a reliable method for filtering the large solid-support materials from the relatively small nucleoside molecules and reactants is required to achieve high yields.

B. Electrowetting on Dielectric (EWOD)

The proposed method for manipulating liquids is performed through EWOD actuation.

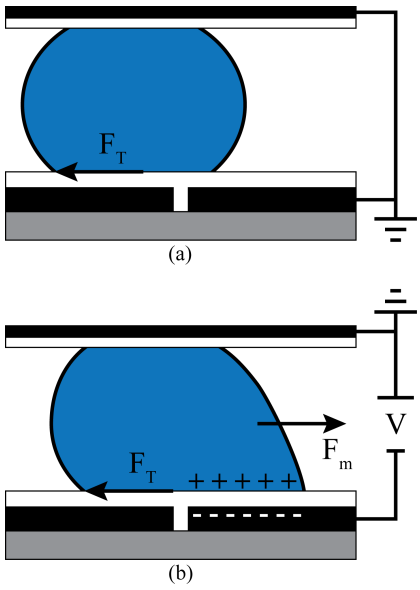

Figure 2. Depiction of EWOD (a) before and (b) after actuation.

EWOD devices consist of a metal electrode, dielectric layer, and hydrophobic coating. As depicted in Figure 5, electrowetting actuation is driven through the application of a voltage on the electrode. As charges orient themselves on the surface of the electrode, charges are also induced in overlapping portions of the droplet. In order to minimize the energy between the liquid-vapor interface and maximize the energy between the liquid-dielectric interface, the contact angle between the liquid-dielectric interface is reduced and a subsequent moving force is created.

$$F_m = \frac{\epsilon_0 \epsilon_R}{2d} V^2 - F_T \tag{1}$$

Equation 1 describes this resultant force (F_m) as a function of: the total capacitance of the dielectric and liquid stack described by the permittivity of free space (ϵ_0), relative permittivity of the stack (ϵ_R), and the total separation between the top and bottom electrodes (d) as well as the frictional force between the liquid-dielectric interface (F_T) [5].

As this device is largely driven by the induced electrostatic forces careful engineering of the capacitance of the dielectric and liquid stack is required. Additionally, as discussed by Lienemann et al. [6], droplet splitting is greatly facilitated by the surface tension resultant from the addition of the top plate. Due to this notion, careful engineering of the total separation between the top and bottom electrodes is required.

C. SU-8 Mechanical Filters

The proposed method for filtering large solid-support materials is performed through the use of SU-8 filters.

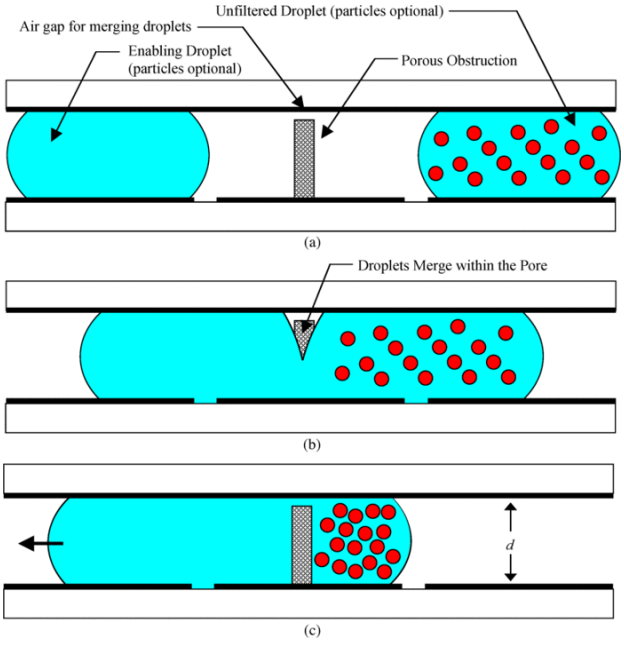

Figure 3. Particle filtration methodology by Schertzer et al.

Figure 3 illustrates the filtration process that was previously performed by Schertzer et al. The process consists of the (a) actuation of an unfiltered droplet and enabling droplet to adjacent electrodes from the porous obstruction filter site, (b) merging of the two droplets at the filter site, and (c) actuation of merged droplet through the filter site. As a relatively basic mechanical filter, the dimensions of the structures are what ultimately decide the filtration performance.

III. Experimental Methodology

A. Device Design and Process Development

Much of the device design was conducted with consideration of previous work by Schertzer et al. With the available custom probe card at the RIT Discrete Microfluidics Laboratory, only 24 pins were available and therefore limited the device in the number of actuation electrodes. Due to this limitation, photolithography masks were designed to fit 6 chips with two devices and 2 chips with one device on a 4-in wafer. Like previous works, each actuation electrode in a device was designed to be 1 mm x 1 mm. Unlike Schertzer et al.,

these electrodes were given a sawtooth edge shape described in the work by Ren et al. in order to allow easier control for droplet movement. Within these designed photomasks, functional features such as thickness monitoring pads, SU-8 pillar information, and SU-8 standoffs were included.

The process flow for these devices also went through revision from the work by Schertzer et al. in order to support the compatible materials and tools in the RIT Semiconductor & Microsystems Fabrication Laboratory. Due to these considerations, devices were fabricated on Corning Eagle XG 2000 wafers rather than microscope slides. It is important to note that these wafers were diced prior to testing.

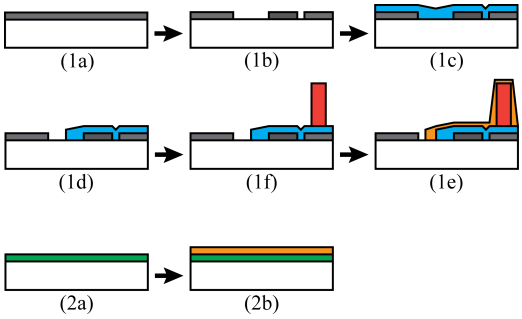

Figure 4. Fabrication process flow of (1a) - (1e) bottom EWOD device and (2a) - (2b) top plate.

Figure 5, encapsulates the revised process used to fabricate the EWOD devices. This cross section primarily focuses on the bare contact electrode and the covered actuation electrode. The following details provide an overview of each process step and the tools that were used:

1) Bottom EWOD Device
   a) Electrode deposition: physical vapor deposition of aluminum and 1% silicon
   b) Electrode patterning: photolithography, aluminum etch, freckle etch, resist strip
   c) Dielectric deposition: plasma enhanced chemical vapor deposition of tetraethyl orthosilicate silicon dioxide
   d) Dielectric patterning: photolithography, pad etch, resist strip
   e) SU-8 Filter patterning: surface plasma cleaning, photolithography
   f) Hydrophobic coating: Teflon AF 2% spin coating, curing
2) Top Plate
   a) Electrode deposition: physical vapor deposition of indium tin oxide
   b) Hydrophobic coating: Teflon AF 2% spin coating, curing

In comparison to previous work by Schertzer et al., this fabrication process is conducted through the use of aluminum and 1% silicon rather than chromium and gold for the electrode material. Additionally, silicon dioxide is used rather than parylene for the dielectric material. After conducting each step in the revised process flow, the top plate is then attached to the bottom EWOD device at the aforementioned SU-8 standoffs to result in the following structure:

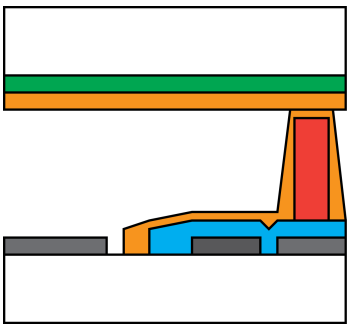

Figure 5. Cross-section of completed device.

Though materials for the electrodes and filters may not be fully compatible with biological particles, this design was fabricated in order to serve as a baseline for future work.

B. Automated Droplet Manipulation

The following hardware was used to perform and observe droplet manipulation:

- NI PXI-5402 14-bit 20 MHz Function Generator
- NI PXI-4072 Digital Multimeter
- TREK PZD700A Amplifier
- NI TB-2636 4x32 Matrix Terminal Block
- Zeiss AxioCam MRm
- Zeiss SteREO Fluorescent Microscope

Droplet manipulation is performed through the generation of a 1 kHz sinusoidal signal with a variable amplitude. This signal is then connected simultaneously to the digital multimeter and also to the amplifier to be able to achieve voltages beyond the limits of the function generator. The output from the amplifier is then connected to the matrix terminal and subsequently connected to the custom probe card in order to be able to deliver the signal to the EWOD device.

Integration of the hardware for automation was conducted using the following software:

- National Instruments Measurement & Automation
- LabVIEW 2014

In order to ensure reliable automation of droplet manipulation, a custom control system is necessary to rapidly connect either the generated signal or ground input to the specified output contact electrode with the interest of ease in prototyping and throughput. With the relatively incompatible logic of the NI hardware control in regard to the available functions in LabVIEW, there was much difficulty in creating a program to support automation.

Figure 6 shows a captured image of the control panel from the LabVIEW program. By simply importing the specified program file, the control system allows for the examination of the entire program file and current step, initialization of NI hardware, modification of generated waveform, approximate measurement of generated waveform, assignment of matrix terminal block inputs and outputs to electrode denominations, and assignment of timings for each step. Furthermore, it is

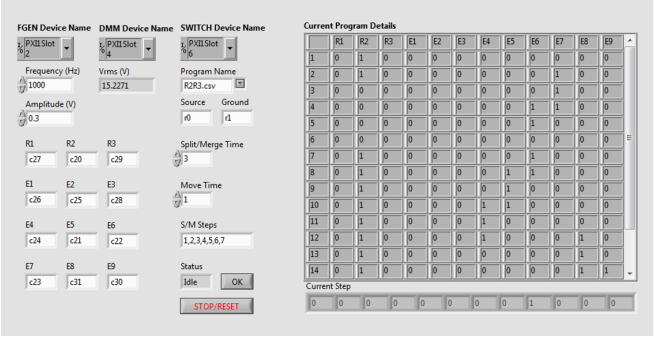

Figure 6. Captured image of custom LabVIEW program for automated droplet manipulation

important to note that this work focused on the manipulation of deionized water in order to serve as a baseline for future work.

IV. Results and Discussion

A. Device Fabrication

With regard to the time that was available for this work, verification of filter fabrication and droplet manipulation automation were conducted separately.

Filters with various dimensions able to filter readily available 40 μm polystyrene solid-support beads were first fabricated. In order to ensure the best filtration performance, isolated trenches with widths smaller than the polystyrene beads were deemed the critical dimension. With an additional desire to maintain reliability in droplet merging at the filter to ultimately enable filtration as well as mechanical stability for repeated use of the device, filter dimensions were varied to achieve either a large number of small filter gaps or a small number of large filter gaps while maintaining feasible fabrication and testing compatibility.

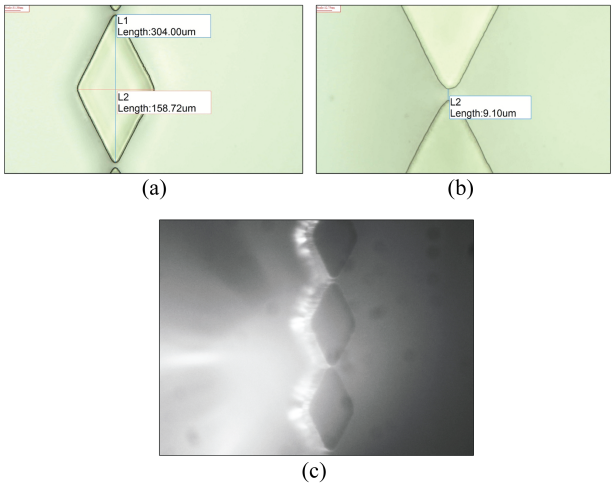

Figure 7. Top-down images of microfabricated SU-8 filters depicting (a) - (b) most reliable dimension and (c) smallest gap filters.

Figure 7 shows top-down images of the fabricated SU-8 filters. In terms of mechanical stability and imaging performance, the most reliable features (a) - (b) that were fabricated were characterized by a filter length of approximately 300 μm, width of approximately 160 μm, height of approximately 118 μm, and a gap of approximately 9 μm. Though these features could easily filter the 40 μm polystyrene beads, a smaller gap distance would be able to support smaller beads. In understanding this, (c) filters with a gap distance of approximately 7 μm were fabricated in order to examine the limits of imaging for this particular SU-8 formulation. Through this process, the fabrication of SU-8 filters compatible with the available solid-support material was verified.

With the verification of the filter fabrication, the latter majority of this work focused on the verification of the droplet manipulation automation.

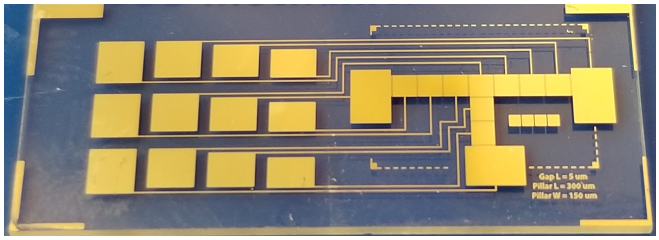

Figure 8. Image of microfabricated bottom device.

Figure 8 shows a captured image of the successfully fabricated bottom device. As mentioned previously, the 12 actuation electrodes, thickness monitoring pads, SU-8 pillar information, and SU-8 standoffs are all initially defined during the electrode patterning step of the process flow. Due to the optically obtrusive use of adhesive spacers used to create the separation between the device, the top plate is not depicted.

B. Manipulation Automation

Manipulation of the droplets went through an initial step through the manual probing of the full EWOD device in order to verify the integrity of the device fabrication. After observing successful electrowetting and manipulation, the process was automated through the use of movement and creation programs written for the LabVIEW control system.

Figure 9 depicts captured key frames during the automated movement of DI water droplets using a 1 kHz sinusoidal signal at 35.5 V_{rms} with a 200 - 250 μm gap. As evident from these images, it is obvious that the movement of DI water droplets was successful. With further examination however, it is clear that the droplets were not created or rather, not separated into smaller quantized volumes, for this movement. At the time of testing, the challenge in droplet creation was much influenced by the difficulty in clean mounting of the top plate as well as the targeting of the gap between the device and top plate.

Figure 10 depicts captured key frames during the automated separation of DI water droplets using a kHz sinusoidal signal at 35.5 V_{rms} with a 100 - 150 μm gap. In comparison to figure 9, the above sequence clear slows the separation of a small droplet from the bottom reservoir. As mentioned previously, this separation was achieved through the variation in the separation between the device and top plate. While

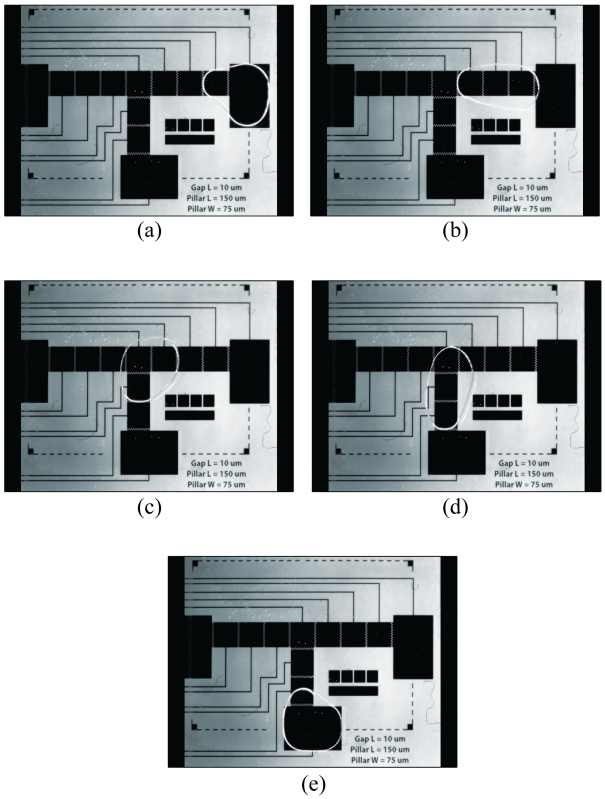

Figure 9. Sequenced images (a) - (e) of successful droplet movement.

these images show successful creation of a droplet, the created droplet volume was unable to provide enough surface area of overlap onto the adjacent electrodes for droplet movement. Though this process however, the need for consistent volume of the created droplet along with an electrode design with more overlap with the previous electrodes was familiarized.

V. Conclusion

Through the course of this work, the previous work done by Schertzer et al., was modified to support the available testing facility and successfully imported for fabrication in the RIT Semiconductor & Microsystems Fabrication Laboratory. With the focus on solid-phase oligonucleotide synthesis, these EWOD devices were successfully designed to support a method for particle filtration as well as key functions such as DI water droplet creation and manipulation. With a desire to allow for rapid prototyping and high throughput, an automation program was written and functionally verified to enable full control and monitoring over the process. While much more work is necessary to be able to successfully and reliably create droplets and subsequently perform movement, works by Nikapitiya et al. [7] and Cho et al. [8] have shown possible solutions for theses challenges. Although these solutions may provide an improvement in automated droplet manipulation, this process must be perfected and characterized for droplet creation reliability, movement velocity, and filtration efficiency

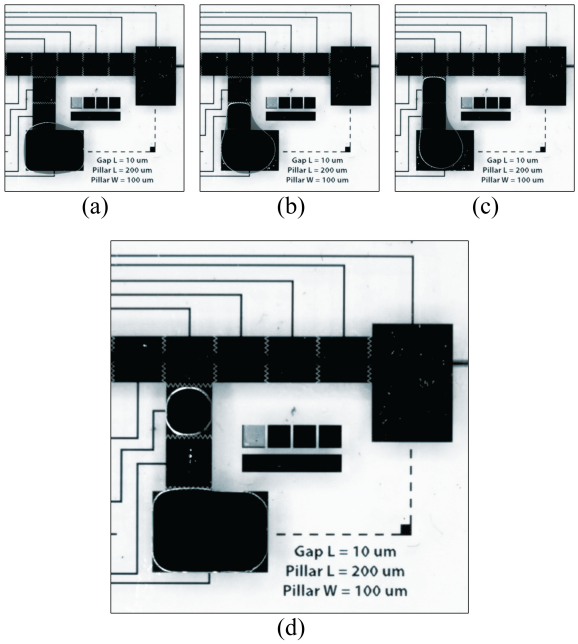

Figure 10. Sequenced images (a) - (d) of successful droplet creation.

prior to the introduction of biological particles for oligonucleotide synthesis. Though many challenges exist for future research, the framework for automated droplet creation and manipulation was created and performed for the first time at the RIT Discrete Microfluidics Laboratory.

References

[1] K. V. I. S. Kaler and R. Prakash, Droplet Microfluidics for Chip-Based Diagnostics, Sensors (Basel), vol. 14, no. 12, pp. 2328323306, Dec. 2014.
[2] C.-C. Lee, T. M. Snyder, and S. R. Quake, A microfluidic oligonucleotide synthesizer, Nucleic Acids Res, vol. 38, no. 8, pp. 25142521, May 2010.
[3] M. J. Schertzer, R. Ben-Mrad, and P. E. Sullivan, Mechanical Filtration of Particles in Electrowetting on Dielectric Devices, Journal of Microelectromechanical Systems, vol. 20, no. 4, pp. 10101015, Aug. 2011.
[4] S. L. Beaucage and M. H. Caruthers, Deoxynucleoside phosphoramiditesA new class of key intermediates for deoxypolynucleotide synthesis, Tetrahedron Letters, vol. 22, no. 20, pp. 18591862, Jan. 1981.
[5] H. Ren, R. B. Fair, M. G. Pollack, and E. J. Shaughnessy, Dynamics of electro-wetting droplet transport, Sensors and Actuators B: Chemical, vol. 87, no. 1, pp. 201206, Nov. 2002.
[6] J. Lienemann, A. Greiner, and J. G. Korvink, Modeling, Simulation, and Optimization of Electrowetting, IEEE Transactions on Computer-Aided Design of Integrated Circuits and Systems, vol. 25, no. 2, pp. 234247, Feb. 2006.
[7] N. Y. J. B. Nikapitiya, S. M. You, and H. Moon, Droplet dispensing and splitting by electrowetting on dielectric digital microfluidics, in 2014 IEEE 27th International Conference on Micro Electro Mechanical Systems (MEMS), 2014, pp. 955958.
[8] S. K. Cho, H. Moon, and C.-J. Kim, Creating, transporting, cutting, and merging liquid droplets by electrowetting-based actuation for digital microfluidic circuits, Journal of Microelectromechanical Systems, vol. 12, no. 1, pp. 7080, Feb. 2003.